# Opposing spin-canting mechanism in single-crystal $LuVO_3$ and $YVO_3$

J.-Q. Yan,* J.-S. Zhou, and J. B. Goodenough
*Texas Materials Institute, ETC 9.102, The University of Texas at Austin, 1 University Station, C2201, Austin, Texas 78712, USA*
(Received 20 April 2005; revised manuscript received 13 July 2005; published 13 September 2005)

A canted-spin ferromagnetic moment **M** parallel to the orthorhombic (*Pbnm*) *a* axis of a $YVO_3$ single crystal changes sign from the direction of a measuring field $\mathbf{H} \leqslant 1$ kOe on warming from 5 K across a first-order orbital-spin reordering temperature $T_{CG}$; the magnetization changes sign again on warming across $T^*$ in the interval $T_{CG} < T^* < T_N$, where $T_N$ is the antiferromagnetic Néel temperature. Although the magnitude of **M** and its sign changes are the same for a sample cooled in a measuring field (FC) and zero-applied field (ZFC) to 5 K, the $\mathbf{M}(T)$ curves differ for warming after FC and ZFC to just above $T_{CG}$; but the sign reversal of **M** occurs at the same $T^*$ with the same measuring field **H**. These unusual features are argued to be the result of two coupled spin-canting mechanisms that oppose one another, an antisymmetric exchange operating on a *c*-axis spin component, and a 90° site anisotropy in the *a*-*b* plane operating on a *b*-axis component of the spin. The relative strength of the antisymmetric exchange increases with decreasing V—O—V bond angle to give a $T^*$ close to a $T_{OO} \approx T_N$ in $LaVO_3$ and no $T^*$ above $T_{CG}$ in $LuVO_3$.

DOI: 10.1103/PhysRevB.72.094412 PACS number(s): 75.60.Jk, 75.20.−g

## INTRODUCTION

The $RVO_3$ perovskites ($R$=rare earth or Y) are a single-valent family in which the octahedral-site $V^{3+}$: $t^2e^0$ ions have only $\pi$-bonding $t$ electrons in an orbitally threefold-degenerate manifold with unquenched orbital angular momentum (azimuthal quantum numbers $m_l = 0, \pm 1$). The $RVO_3$ perovskites with $R$=La, Y, Lu are of particular interest since the $R^{3+}$ ions carry no moment either to obscure the magnetic behavior of the $VO_3$ array or to interact with it. A single-crystal study of $YVO_3$ has shown it undergoes a second-order orbital order-disorder transition at $T_{OO}$=200 K, a second-order antiferromagnetic order-disorder transition at $T_N$=116 K, and a first-order orbital and spin reordering transition at $T_{CG}$=77 K.[1] A similar sequence of transitions occurs in $LuVO_3$.[2] In the interval $T_{CG} < T < T_{OO}$, the orbital ordering stabilizes alternately empty *yz* and *zx* orbitals on neighboring $V^{3+}$ ions (*G*-type orbital order), which gives a tetragonal ($c_s/a_s > 1$) site distortion with a long (V—O) bond in the *a*-*b* plane of the orthorhombic (*Pbnm* space-group) structure.[3] The site distortion lowers the orbital angular momentum by stabilizing the two $t^2$ electrons in the $m_l = \pm 1$ orbitals; the $m_l = 0$ orbital is empty, as should be expected for a $T_{OO} > T_N$ since spin-orbit coupling would suppress cooperative orbital ordering in a paramagnetic phase. In the interval $T_{CG} < T < T_N$, the spin ordering consists of ferromagnetic V—O—V chains that are coupled antiparallel to one another by antiferromagnetic V—O—V interactions in the *a*-*b* plane.[3] This *Type-C* antiferromagnetic order conforms to the Goodenough-Kanamori superexchange rules: the *c*-axis $yz^1$-O-$yz^0$ and $zx^1$-O-$zx^0$ interactions are both ferromagnetic; the antiferromagnetic $xy^1$-O-$xy^1$ interactions in the *a*-*b* plane dominate a weaker $yz^1$-O-$yz^0$ or $zx^1$-O-$zx^0$ interaction. Below $T_{CG}$, *c*-axis chains of empty *yz* or empty *zx* orbitals alternate with one another in the *a*-*b* plane (*C*-type orbital order) to give antiferromagnetic $yz^1$-O-$yz^1$ or $zx^1$-O-$zx^1$ coupling along the *c* axis; the anitferromagnetic coupling in the *a*-*b* plane remains the same to give *Type-G* antiferromagnetic order.[3] In both antiferromagnetic phases, spin canting gives a weak ferromagnetic component parallel to the orthorhombic *a* axis.

A remarkable phenomenon has been observed in $YVO_3$.[1,4] On cooling through $T_N$ in a measuring field **H** oriented parallel to the *a* axis of the crystal (FC), the weak ferromagnetic moment **M** is initially aligned with **H**, but it changes sign to oppose **H** on further cooling in the interval $T_{CG} < T < T_N$, jumping back to alignment with **H** on cooling through $T_{CG}$. On reheating from 5 K in the measuring field, the magnetization with its sign changes is retraced. Moreover, the same **M** was retraced on heating in the measuring field after the sample had been cooled in a nominal [small remanent field in the superconducting quantum interference device (SQUID)] zero-applied field **H** (ZFC). Like $YVO_3$ in the interval $T_{CG} < T_C < T_N$, $LaVO_3$ has *G*-type orbital order and Type-*C* antiferromagnetic order below $T_{OO} \approx T_N$;[2] however, in this case, the weak ferromagnetism parallel to the *a* axis changes sign on cooling only a few degrees below $T_{OO} \approx T_N$ to oppose the magnetizing field.[5–7] Ren *et al.*[1,4] have correctly argued that, in the case of $YVO_3$, a canting by a magnetocrystalline anisotropy must oppose a canting by antisymmetric exchange, but they did not specify the origin of the canting by magnetocrystalline anisotropy and they assumed that the canting by antisymmetric exchange is dominant at the lower temperatures.

In order to explore this phenomenon further, we have measured the magnetic properties of a single crystal of $LuVO_3$ for comparison and we have made additional measurements on a $YVO_3$ crystal. Experimentally, we find that the temperature $T^*$ below which the magnetization is reversed to oppose the magnetizing field decreases from $LaVO_3$ to $YVO_3$ to $LuVO_3$ as the V—O—V bond angle decreases and that $YVO_3$ exhibits different FC and ZFC $\chi(T)$ curves, but the same $T^*$, for the same measuring field when cooled to the interval $T_{CG} < T < T^*$, whereas there is no difference in the $\chi(T)$ curves when cooled to below $T_{CG}$. We identify the two competing spin-canting mechanisms in the

 

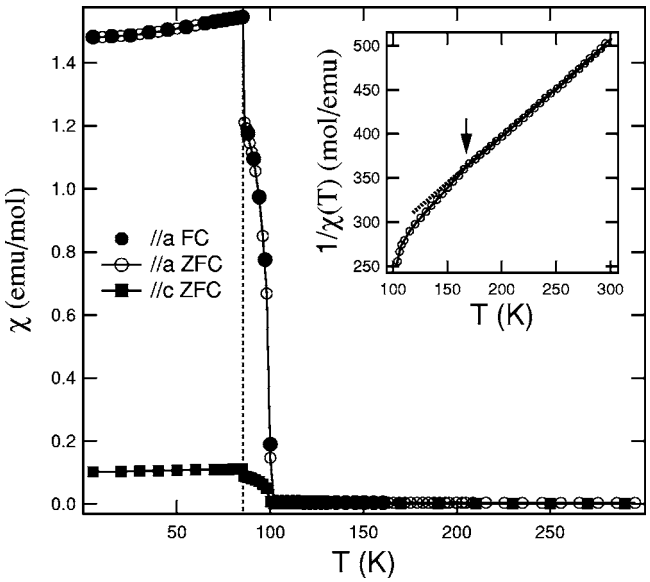


FIG. 1. Temperature dependence of magnetic susceptibility of $LuVO_3$ single crystals along different directions measured at 50 Oe. $\chi(T)$ curve along the $b$ axis overlaps with that along the $c$ axis. Inset highlights the slope change of the $1/\chi(T)$ curve (measured at 5 T) at $T_{OO}$ as denoted by a solid arrow.

phase with Type-$C$ antiferromagnetic order ($T_{CG}<T<T_N$) that are opposed to one another; since spin-orbit coupling is responsible for both an antisymmetric exchange coupling of a spin component parallel to the $c$ axis and a 90° site anisotropy in the basal plane canting a $b$-axis spin component, the opposed canting mechanisms are coupled to one another. Only the antisymmetric exchange $\mathbf{D}_{ij}\cdot\mathbf{S}_i\times\mathbf{S}_j$ is operative below $T_{CG}$ where there is no $b$-axis component of the spin, and the direction of $\mathbf{D}_{ij}$ is not reversed on crossing $T_{CG}$.

## EXPERIMENTAL

Single crystals of $LuVO_3$ and $YVO_3$ with a typical size of ~4 mm in diameter and ~6 mm long were grown by the floating-zone technique in an IR image furnace as reported elsewhere.[8] A large thermoelectric power ($\alpha>500$ $\mu$V/K) at room temperature implies a nearly stoichiometric oxygen content. The Laue diffraction pattern shows clear, round spots signaling a good crystal quality. The as-grown single crystals were single-phase to x-ray powder diffraction made on ground portions of a crystal; all peaks could be indexed with the orthorhombic *Pbnm* symmetry. The room-temperature lattice parameters, determined by x-ray powder diffraction with fine Si powder as the internal standard, were $a=5.209$ Å, $b=5.564$ Å, and $c=7.531$ Å for $LuVO_3$ in good agreement with those reported in the literature.[9] The single crystals were well oriented within an error of less than 1°. Magnetic properties were measured with a Quantum Design SQUID in the temperature range $5\leqslant T\leqslant 700$ K.

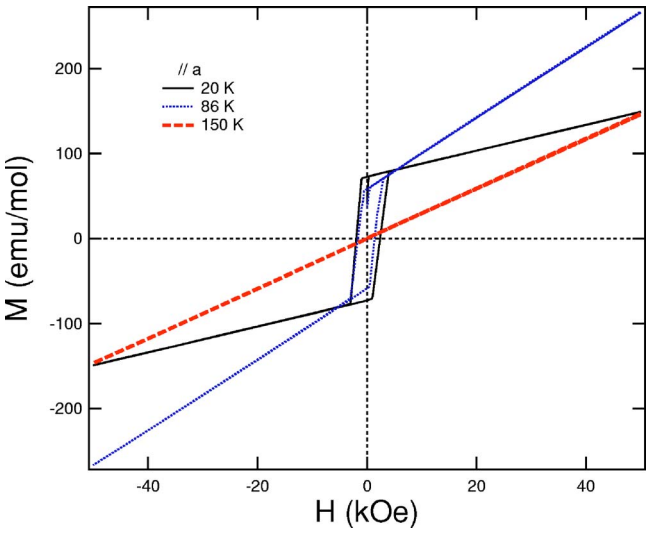


FIG. 2. (Color online) $M(H)$ curves measured at different temperatures for $LuVO_3$ along the $a$ axis.

## RESULTS

Figure 1 shows the temperature dependence of the molar magnetic susceptibility $\chi(T)$ of a single crystal of $LuVO_3$ taken with $H=50$ Oe along the different crystallographic axes; the inset shows the inverse susceptibility $1/\chi(T)$ taken with $H=5$ T along the $a$ axis of space group *Pbnm*. The following features are noteworthy:

(1) A change of slope in $1/\chi(T)$ is found at $T_{OO}$ in $RVO_3$ compounds.[4] In our $LuVO_3$ crystal, this change occurs at $T_{OO}=170$ K, which is to be compared with $T_{OO}=200$ K in $YVO_3$.

(2) A fit with the Curie-Weiss law $\chi(T)=C/(T-\theta)$ above $T_{OO}$ gives a $\mu_{eff}=2.74\mu_B$, which approaches the spin-only value of $2.83\mu_B$ for $S=1$ and $\theta=-180$ K.

(3) From $\chi(T)$, a weak canted-spin ferromagnetic component of the magnetization sets in along the $a$ axis below $T_N=102$ K, which is to be compared with $T_N=116$ K in $YVO_3$.

(4) The sharp rise in $\chi(T)$ on cooling below $T_N$ marks the first-order orbital reordering temperature $T_{CG}=85$ K, which is to be compared with $T_{CG}=77$ K in $YVO_3$.

(5) On cycling between 5 K and room temperature, the $\chi(T)$ curves taken on warming are the same after cooling in zero-applied field (ZFC) and in the measuring field (FC). This behavior is similar to that found for $YVO_3$.

Figure 2 shows three $M(H)$ curves between −5 T and +5 T with $\mathbf{H}$ along the $a$ axis of $LuVO_3$ taken at 20 K $<T_{CG}$, $T_{CG}<86$ K $<T_N$, and $T_N<150$ K $<T_{OO}$. Below $T_N$, the $M(H)$ curves exhibit a coercivity $H_C\approx 2$ kOe and a finite remanence. The knee of the hysteresis loop is sharply defined at an $H_n\approx\pm 1$ kOe.

The $\chi(T)$ curve for $YVO_3$ differs from that of Fig. 1 by changing from positive to negative on warming through $T_{CG}$ and returning monotonically to positive again on warming across a $T^*$ before dropping to a low value at $T_N$. The temperature difference $T_N-T_{CG}=17$ K in $LuVO_3$ compared to 39 K in $YVO_3$ is small for the onset of a negative magnetization as found in the interval $T_{CG}<T<T_N$ in $YVO_3$. Therefore, we performed the experiment shown in Fig. 3.

The solid circles in Fig. 3 show the magnetization obtained on cooling to 92 K in a field $H=50$ Oe applied parallel to the $a$ axis of the $LuVO_3$ crystal. At 92 K, a high mag-

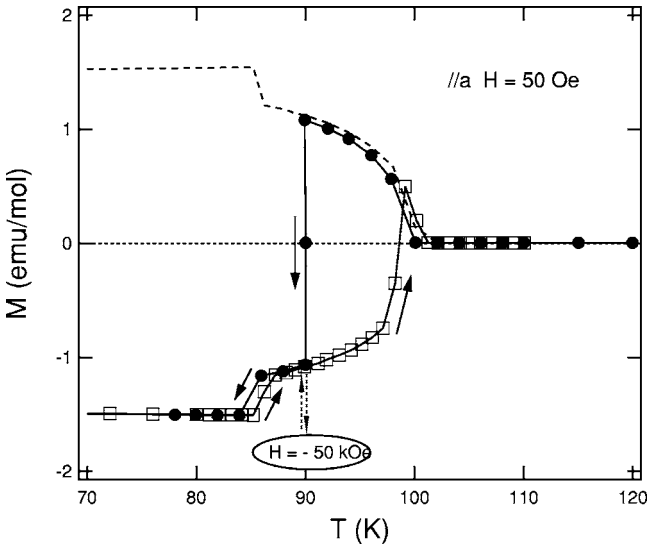


FIG. 3. Temperature dependence of magnetization along the *a* axis. The dashed line shows the magnetization measured at 50 Oe in a normal FC mode. The curve with open circles was measured at 50 Oe while cooling; at 92 K, a field of −50 kOe was applied to flip the canted spins and then the field was changed back to 50 Oe. The curve with open squares was measured upon warming after the temperature had reached 5 K.

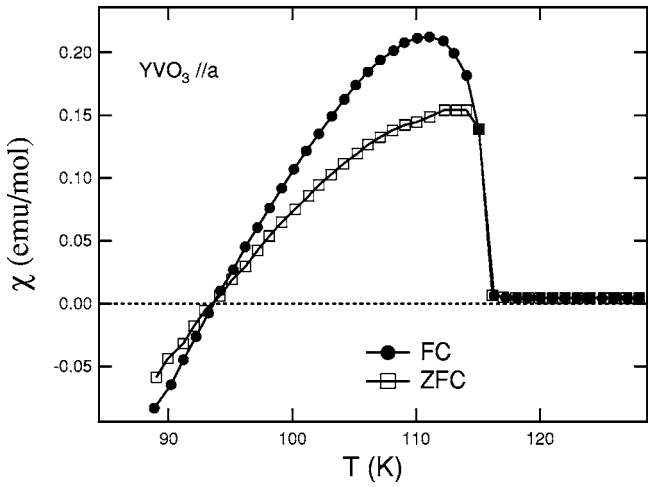


FIG. 4. Temperature dependence of the magnetic susceptibility of a $YVO_3$ crystal measured in FC and ZFC modes in a field of 100 Oe parallel to the *a* axis. During the measurement, the temperature was carefully controlled to be above $T_{CG}$.

netic field of −50 kOe was applied to reverse the magnetization. Then the field was changed back to +50 Oe and the magnetization remained negative on cooling to 5 K. It remained negative on warming up until just below $T_N$, open squares, with only a small thermal hysteresis at $T_{CG}$. Unlike $YVO_3$, there is no reversal of the sign of the magnetization on cooling through $T_{CG}$; the $M(T)<0$ mirrors the $M(T)>0$ obtained on cooling to 5 K in 50 Oe without the application of a reverse field of −50 kOe at $T=92$ K.

The fact that the FC and ZFC $\chi(T)$ curves overlap on cycling between 5 K and room temperature in both $LuVO_3$ and $YVO_3$ is unusual. Therefore, we studied whether a difference in the FC and ZFC curves would be found in $YVO_3$ if the crystal was cooled to $T_{CG}<89$ K$<T_N$. Figure 4 shows that the FC curve gives the larger $\chi(T)$, but that both curves change sign at the same temperature $T^*=94$ K.

Figure 5 shows the evolution with time of the magnetization of the $YVO_3$ crystal ZFC to $T_{CG}<82$ K$<T^*$ measured at a small field of 10 Oe after a larger field was applied. The larger magnetic field had been applied perpendicular to the *c* axis, and the field was changed to +10 Oe immediately after the larger field had become stable. Three larger fields were used; +25 Oe left the magnetization in opposition to the field, 2 T and 5 T switched the magnetization and the magnetization stayed to be positive even after the field was removed. In all cases, the magnitude of the magnetization initially dropped and then increased to a stable value after a longer relaxation time. The increasing magnetization with time could be fitted with the following equation:

$$M = M_0 + B\exp(-t/\tau),$$

where $\tau$ is the relaxation time and $M_0$ and $B$ are constants. The parameters are shown in Table I. Obviously, the relaxation time is the same for all three experiments, which indicates the same energy barrier for the spin relaxation.

## DISCUSSION

The change of slope of $1/\chi(T)$ of $LuVO_3$ at $T_{OO}$ reflects either a change in the magnitude of the atomic moment or a change in the strength of the interatomic exchange interactions. Given a $\mu_{\text{eff}}$ close to the spin-only value at temperatures $T>T_{OO}$ and an orbital ordering that reduces any orbital angular momentum contribution to $\mu_{\text{eff}}$, the latter change should be the dominant feature. Orbital order introduces a *c*-axis ferromagnetic component into the interatomic exchange interactions, which must increase the Weiss constant $\theta$. However, the orbital order-disorder transition at $T_{OO}$ is second order, which means a continuous change in $1/\chi(T)$ across $T_{OO}$. The result is a $1/\chi(T)$ curve that shows a progressively larger lowering with decreasing temperature from its value as extrapolated from $T>T_{OO}$ until it falls abruptly to a low value on cooling through $T_N$ because of the appearance of a canted-spin ferromagnetic component below $T_N$.

In the orthorhombic *Pbnm* structure, the $VO_{6/2}$ octahedra rotate cooperatively about the *b* axis and the Dzyaloshinskii vector $\mathbf{D}_{ij}$ is parallel to the *b* axis. The spin configurations in the interval $T_{CG}<T<T_N$ that have been reported by different groups on the basis that their neutron-diffraction data differ from one another, but Blake *et al.*[3] and Ulrich *et al.*[10] have both reported a dominant *c*-axis spin with a ferromagnetic *a*-axis canting below $T_{CG}$ and an important spin component along the *b* axis as well as the *c* axis in the interval $T_{CG}<T<T_N$.

Below $T_{CG}$, the Type-*G* antiferromagnetic component of the spins is along the *c* axis;[3] in this case, both the antisymmetric exchange term $\mathbf{D}_{ij}\cdot\mathbf{S}_i\times\mathbf{S}_j$ and a site anisotropy retaining the spin direction parallel to a cooperatively rotated (V—O) bond give a ferromagnetic canted-spin component parallel to the *a* axis. The site-anisotropy canting is illus-

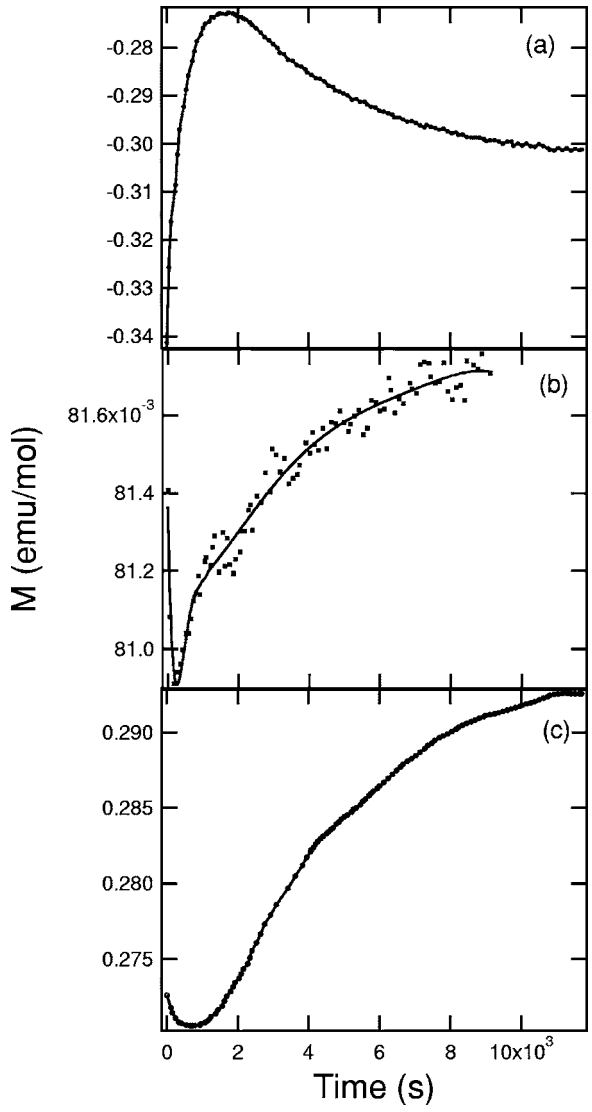


FIG. 5. Time dependence of magnetization of a $YVO_3$ crystal at 82 K measured in 10 Oe after a large field was applied. The large magnetic fields used were 25 Oe (a), 2 T, (b) and 5 T (c).

trated in Fig. 6(a). The small *a*-axis component is also reflected in the *c*-axis susceptibility of Fig. 1.

In the interval $T_{CG} < T < T_N$, on the other hand, only the $\mathbf{D}_{ij} \cdot \mathbf{S}_i \times \mathbf{S}_j$ term gives a component along the *a* axis as a result of a Type-*C* antiferromagnetic component along the *c* axis in $YVO_3$. As illustrated in Fig. 6(b), the cooperative rotations of the $VO_{6/2}$ octahedra give canted-spin components of the *c*-axis spin component that cancel one another. Moreover, the significant spin-component parallel to the *b* axis from neutron-diffraction data[3,10] is unaffected by cooperative rotations of the $VO_{6/2}$ octahedra about the *b* axis. Therefore, we must look for an alternative mechanism for the introduction of a canted-spin component parallel to the *a* axis that opposes the antisymmetric exchange term.

TABLE I. The *M* versus time curve fitting parameters.

| Field | $M_0$ | *B* | $\tau$ |
|---|---|---|---|
| 25 Oe | −0.3058(5) | 0.0500(4) | 0.000222(6) |
| 2 T | 0.081 81(4) | −0.000 82(2) | 0.000 25(3) |
| 5 T | 0.2956(1) | −0.0337(1) | 0.000 221(3) |

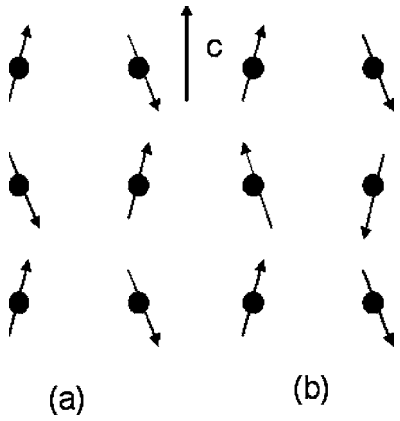


FIG. 6. Nearest-neighbor tilting of the *c*-axis component of the spins along *a* axis by cooperative $VO_{6/2}$ site rotations (a) for Type-*G* and (b) for Type-*C* antiferromagnetic order of the spin component along the *c* axis. Arrows indicate spins, while solid circles denote V sites.

A component of the site easy axis in the *a*-*b* plane would reflect the orbital order, which gives a site distortion to tetragonal $c_s/a_s > 1$ symmetry. An easy axis perpendicular to the site tetragonal axis would be alternately in the pseudocubic (100) and (010) planes. Although this sign of the distortion lowers the orbital-angular momentum, it does not suppress it completely, and the component of the easy spin axis in the *a*-*b* plane for each $V^{3+}$ ion would be oriented alternately along the pseudocubic [100] and [010] axes, which are at 90° to one another. The symmetric antiferromagnetic exchange interactions in the *a*-*b* planes would align the spins antiparallel to one another, and the best compromise between the stronger exchange and weaker anisotropy energies would be a major spin component along the site rotation axis, i.e., the orthorhombic *b* axis, with a canting due to the site anisotropy to give a ferromagnetic component along the *a* axis. An observed major spin component along the *b*-axis is, therefore, consistent with a net ferromagnetic component along the *a* axis. Available experimental data for all $RVO_3$ perovskites with *G*-type orbital order are consistent with an antiparallel coupling of the two contributions to the canted-spin ferromagnetic component parallel to the *a* axis. However, why the anisotropy-induced spin canting from the *b* axis component of the spins opposes the spin canting arising from the antisymmetric exchange between the *c*-axis component of the spins needs to be examined.

To answer this question, we note that both the Dzyaloshinskii vector $\mathbf{D}_{ij}$ and the site anisotropy depend upon spin-orbit coupling. Examination of Moriya's[11] expression for $\mathbf{D}_{ij}$ shows it is proportional to $-\lambda$ whereas the site anisotropy is proportional to $+\lambda$, where $\lambda$ is the spin-orbit coupling parameter. We conclude that once the direction of $\mathbf{D}_{ij}$ is determined by an applied magnetic field, the sense of rotation of the electrons around the axis of the field is fixed and the direction of the orbital magnetic moment is determined

so as to orient the anisotropy-induced spin canting in opposition to that induced by $\mathbf{D}_{ij}$.

Competition between two canted-spin ferromagnetic components parallel to the *a* axis accounts for the change of sign of the magnetization in the interval $T_{CG}<T<T_N$ of $YVO_3$. The narrower range of this temperature interval in $LuVO_3$ cannot, by itself, account for the absence of a sign reversal of $\chi(T)$ in Fig. 1 since the temperature interval is large enough for some reduction of the magnetization if the two competing spin-canting mechanisms were of the same relative strength as found in $YVO_3$. The cooperative spin rotations in $LuVO_3$ have a component about the *c* axis as well as about the *b* axis,[3] and this rotation would give a weak ferromagnetic component along the *a* axis in the same direction as the Dzialoshinskii canting. We conclude that the strength of the antisymmetric exchange relative to that of the anisotropy canting must be considerably greater in $LuVO_3$ just as it is greater in $YVO_3$ than in $LaVO_3$ and that the component of the site rotations about the *c* axis in $LuVO_3$ enhances this trend. This observation is consistent with the fact that the magnitude of $\mathbf{D}_{ij}$ increases as the V—O—V angle decreases and with a smaller site distortion in $LuVO_3$ than in $YVO_3$, which decreases the strength of the anisotropy canting. In $YVO_3$, the sign of $\chi(T)$ returns to positive on cooling through $T_{CG}$, and in $LuVO_3$ a $\chi(T)>0$ increases abruptly at $T_{CG}$. Quite remarkable is the fact that on heating and cooling in a modest measuring field $H\leqslant 1$ kOe or heating in the same measuring field after a ZFC or a FC gives an identical $\chi(T)$ curve in both $LuVO_3$ and $YVO_3$. A small remanent field in the SQUID magnetometer is sufficient to determine the direction of the precessional motion of $\boldsymbol{\mu}_J$ about the field axis in a nominal ZFC run;[12] and once the direction of $\mathbf{D}_{ij}$ is established, it is fixed so long as the measuring field is not high enough to reverse the direction of the precession. The direction of $\mathbf{D}_{ij}$ can be seen to be unchanged by the orbital reorientation at $T_{CG}$.

The hysteresis loops of Fig. 2 show a coercivity of about 2 kOe and a sharp knee of the loop at an $H_n\approx\pm 1$ kOe for both 20 K$<T_{CG}$ and $T_{CG}<86$ K$<T_N$. Nucleation and/or growth of the reverse domains in $LuVO_3$ requires a negative field $|H-H_n|>0$, and a sharp knee with a relatively square *M*-*H* loop indicates that domain walls are mobile in the fields $H>H_n$ that nucleate the domains of reverse magnetization.

A field **H** parallel to the *a* axis exerts a large torque on spins having a major component in the *b*-*c* plane; therefore, the magnetization increases linearly with **H**, failing to saturate at 5 T. The slope of the $M(H)$ curve is larger the greater the net moment **m** experiencing the torque $\boldsymbol{\tau}=\mathbf{m}\times\mathbf{H}$ and the weaker the net exchange interactions coupling the **m** antiparallel. With *C*-type antiferromagnetic order in the interval $T_{CG}<T<T_N$, ferromagnetic coupling along the *c* axis gives a large effective **m** and antiferromagnetic exchange is restricted to the *a*-*b* plane. Consequently, the slope of the $M(H)$ curve at $H>H_C$ is larger than that for the paramagnetic phase at 150 K because of the larger effective **m**. With *G*-type antiferromagnetic order below $T_{CG}$, order reduces **m** to a single $V^{3+}$ ion as in the paramagnetic phase, and a stronger three-dimensional (3D) V—O—V antiferromagnetic coupling below $T_N$ reduces the $M(H)$ slope at $H>H_C$ to less than that of the paramagnetic phase.

Figure 3 shows that the application of a reverse field of −50 kOe in the range $T_{CG}<T<T_N$ is able to reverse the sign of $\mathbf{D}_{ij}$. Since $\mathbf{D}_{ij}$ does not change sign on cooling through $T_{CG}$ and the antisymmetric exchange remains dominant to $T_{CG}$ in $LuVO_3$, the magnetization does not change sign on cooling through $T_{CG}$ as is found in $YVO_3$ on cooling in an $H<1$ kOe. The sign reversal on heating to $T_N$ in an $H=+50$ Oe after applying a field of −50 kOe at 90 K shows that the coercive field $H_c$ required to switch the magnetization decreases to below 50 Oe as *T* approaches $T_N$.

The observation in Fig. 4 of a $T^*=94$ K that is the same whether the sample is ZFC or FC to 89 K$>T_{CG}$ even though the two $\chi(T)$ curves differ, shows that the spin reversal of the magnetization is intrinsic; the differing $\chi(T)$ curves reflect the presence of magnetic domains in the ZFC sample and a growth of the favorably oriented domains on cooling in a magnetic field. Apparently, on cooling across $T_{CG}$, the plasticity of the orbital reorientation allows the $\mathbf{D}_{ij}$ to favorably orient all of the ZFC sample below $T_{CG}$ as the magnetization reverses sign on crossing $T_{CG}$ since the FC and ZFC $\chi(T)$ curves are the same if the sample is cooled below $T_{CG}$.

Figure 5 shows the evolution of the magnetization with time from removal of a larger magnetic field $H_a$ applied perpendicular to the *c* axis of a $YVO_3$ crystal that had been ZFC to 82 K; the magnetization $M(t)$ was obtained in a measuring field $H=10$ Oe applied in the same direction as $H_a$. Two relaxation times are apparent; an initial relaxation to a smaller or more negative *M* followed by a longer relaxation period to a more positive or less negative *M*. The initial relaxation after removal of the larger $H_a>0$ field reflects relaxation of the domain walls and/or spins that overshoot their equilibrium positions in an $H=10$ Oe from those in an $H_a>10$ Oe. The second, slower relaxation appears to reflect a damped return of domain-wall and/or spin oscillations to their new equilibrium positions. Since the relaxation times are similar for $H_a=25$ Oe, 20 kOe, and 50 kOe, we conclude that these relaxation times are independent of the times for nucleation and growth of the domains of reverse $\mathbf{D}_{ij}$ vectors in fields $H_a>10$ Oe.

## CONCLUSIONS

We have discussed three origins of a canting of antiferromagnetic spins to give a weak *a*-axis ferromagnetic moment: (1) cooperative site rotations about the orthorhombic *b* axis (*Pbnm*) cant a *c*-axis component of the spin; but these site rotations give a net ferromagnetic spin-component parallel to the *a* axis only for *G*-type antiferromagnetic order, i.e., below $T_{CG}$; (2) antisymmetric exchange $\mathbf{D}_{ij}\cdot\mathbf{S}_i\times\mathbf{S}_j$ operating on a *c*-axis spin; and (3) a 90° component of the site anisotropy in the *a*-*b* plane operating on a *b*-axis spin. In the interval $T_{CG}<T<T_N$ where the *C*-type magnetic order has spin components along both the *b* and *c* axes, canting (2) and (3) are operative, but they are in competition with one another. The direction of $\mathbf{D}_{ij}$ is determined by a small applied field **H** on cooling through $T_N$, but the anisotropy term becomes stronger at lower temperatures and reverses the sign

of the weak ferromagnetism parallel to the *a* axis in the interval $T_{CG}<T<T_N$ of $YVO_3$. A larger V—O—V bond angle in $LaVO_3$ weakens the antisymmetric exchange, and the anisotropy term reverses the magnetization only a few degrees below $T_{OO}\approx T_N$; but a *c*-axis component to the cooperative site rotations and smaller V—O—V bond angle in $LuVO_3$ than in $YVO_3$ strengthens the effective antisymmetric exchange relative to the anisotropy canting, and the temperature interval $T_{CG}<T<T_N$ is not large enough for a sign reversal in $LuVO_3$. With only a *c*-axis component of the spin in the Type-*G* antiferromagnetic phase below $T_{CG}$, the $\mathbf{D}_{ij}\cdot\mathbf{S}_i\times\mathbf{S}_j$ term and the cooperative $VO_{6/2}$ rotations cant the spins in the same direction along the *a* axis, and the magnetization is aligned by $\mathbf{D}_{ij}$. The direction of $\mathbf{D}_{ij}$ is determined by a small remanent field in the SQUID magnetometer at $T_N$. The sign of $\mathbf{D}_{ij}$ does not change on traversing the first-order orbital-spin reorientation at $T_{CG}$.

## ACKNOWLEDGMENTS

The NSF and the Robert A. Welch Foundation of Houston, Texas are thanked for financial support.

*Corresponding author. Present address: Ames Lab, Neutron and X-ray Group, A524 Physics, Ames, IA 50011.

[1] Y. Ren, T. T. M. Palstra, D. I. Khomskii, E. Pellegrin, A. A. Nugroho, A. A. Menovsky, and G. A. Sawatzky, Nature (London) **396**, 441 (1998).

[2] S. Miyasaka, Y. Okimoto, M. Iwama, and Y. Tokura, Phys. Rev. B **68**, 100406(R) (2003).

[3] G. R. Blake, T. T. M. Palstra, Y. Ren, A. A. Nogruho, and A. A. Menovshy, Phys. Rev. B **65**, 174112 (2002).

[4] Y. Ren, T. T. M. Palstra, D. I. Khomskii, A. A. Nogruho, A. A. Menovsky, and G. A. Sawatzky, Phys. Rev. B **62**, 6577 (2000).

[5] N. Shirakawa and M. Ishihara, Jpn. J. Appl. Phys., Part 2 **30**, L755 (1991).

[6] A. V. Mahajan, D. C. Johnston, D. R. Jorgeson, and F. Borsa, Physica C **185-189**, 1095 (1991).

[7] H. C. Nguyen and J. B. Goodenough, Phys. Rev. B **52**, 324 (1995).

[8] J.-Q. Yan, J.-S. Zhou, and J. B. Goodenough, Phys. Rev. Lett. **93**, 235901 (2004).

[9] A. Munoz, J. A. Alonso, M. T. Casais, M. J. Martinez-Lope, J. L. Martinez, and M. T. Fernandez-Diaz, Chem. Mater. **16**, 1544 (2004).

[10] C. Ulrich, G. Khaliullin, J. Sirker, M. Reehuis, M. Ohl, S. Miyasaka, Y. Tokura, and B. Keimer, Phys. Rev. Lett. **91**, 257202 (2003).

[11] T. Moriya, Phys. Rev. **120**, 91 (1960).

[12] J.-Q. Yan, J.-S. Zhou, and J. B. Goodenough (unpublished).